Supplement of Atmos. Chem. Phys., 17, 2009–2033, 2017
http://www.atmos-chem-phys.net/17/2009/2017/
doi:10.5194/acp-17-2009-2017-supplement

Atmospheric Chemistry and Physics
Open Access

Supplement of

Sources and atmospheric processing of winter aerosols in Seoul, Korea: insights from real-time measurements using a high-resolution aerosol mass spectrometer

H. Kim et al.

Correspondence to: Qi Zhang (dkwzhang@ucdavis.edu)

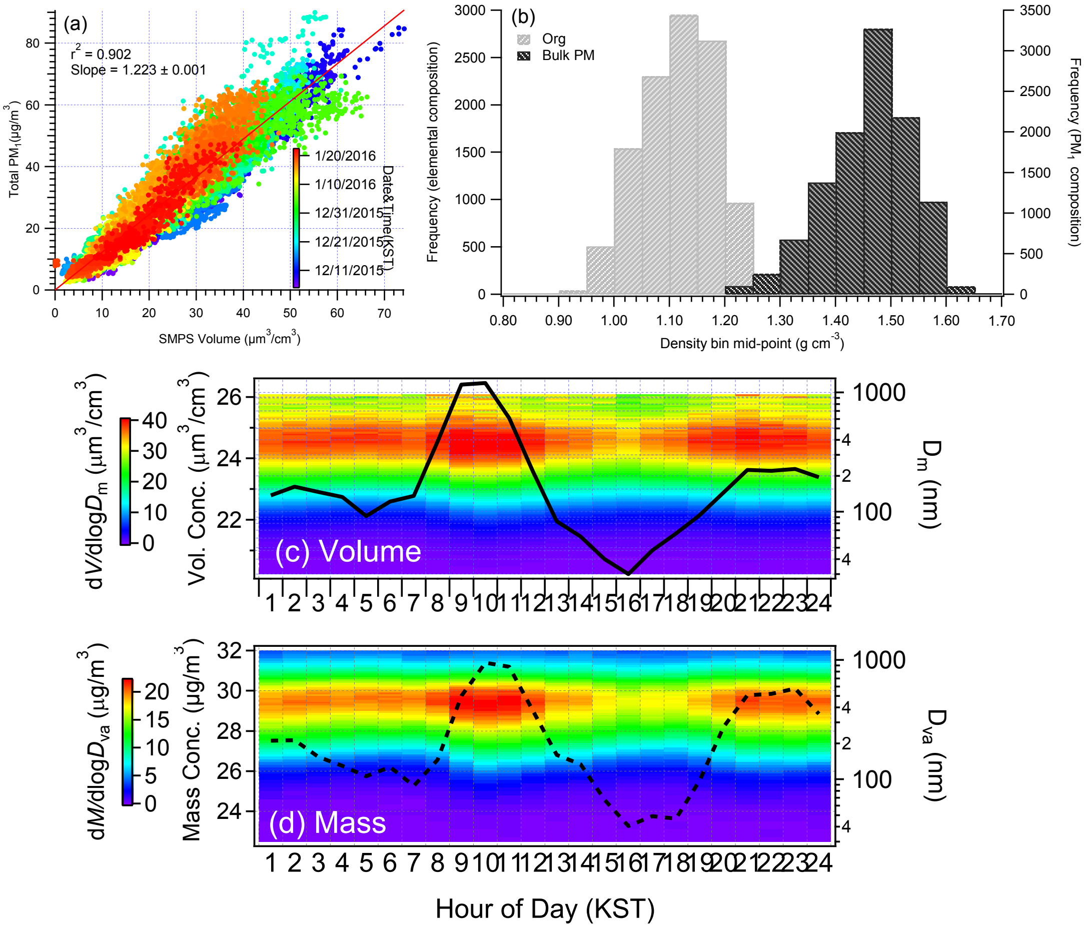

Figure S1. **(a)** Scatter plot of the total PM_1 mass (NR-PM_1 plus BC) versus SMPS volume, where the NR-PM_1 has been corrected using a time- and composition-dependent collection efficiency (Middlebrook et al., 2012); **(b)** histogram of organic density calculated measured elemental ratios (Kuwata et al., 2012), averaging 1.12 g cm^{-3} and bulk aerosol density estimated from the measured chemical composition in this study (Zhang et al., 2005), averaging 1.46 g cm^{-3}. **(c)** Diurnal variations of the size distribution of volume from the SMPS (in mobility diameter, D_m) and **(d)** NR-PM_1 mass from the AMS (in vacuum aerodynamic diameter, D_{va}).

Table S1. Comparison of the O/C, H/C, and OM/OC ratios of total OA and the six OA factors identified from PMF analysis calculated using the Aiken-Ambient method (Aiken et al., 2008) and the improved Canagaratna-Ambient method (Canagaratna et al., 2015).

Species	Ratio	Aiken-Ambient	Canagaratna-Ambient
OA	O/C	0.29	0.37
	H/C	1.62	1.79
	OM/OC	1.54	1.67
HOA	O/C	0.05	0.06
	H/C	2.04	2.21
	OM/OC	1.24	1.27
COA	O/C	0.11	0.14
	H/C	1.76	1.89
	OM/OC	1.30	1.36
BBOA	O/C	0.26	0.34
	H/C	1.56	1.74
	OM/OC	1.49	1.61
SVOOA	O/C	0.43	0.56
	H/C	1.70	1.90
	OM/OC	1.74	1.94
LVOOA	O/C	0.52	0.68
	H/C	1.42	1.61
	OM/OC	1.84	2.07

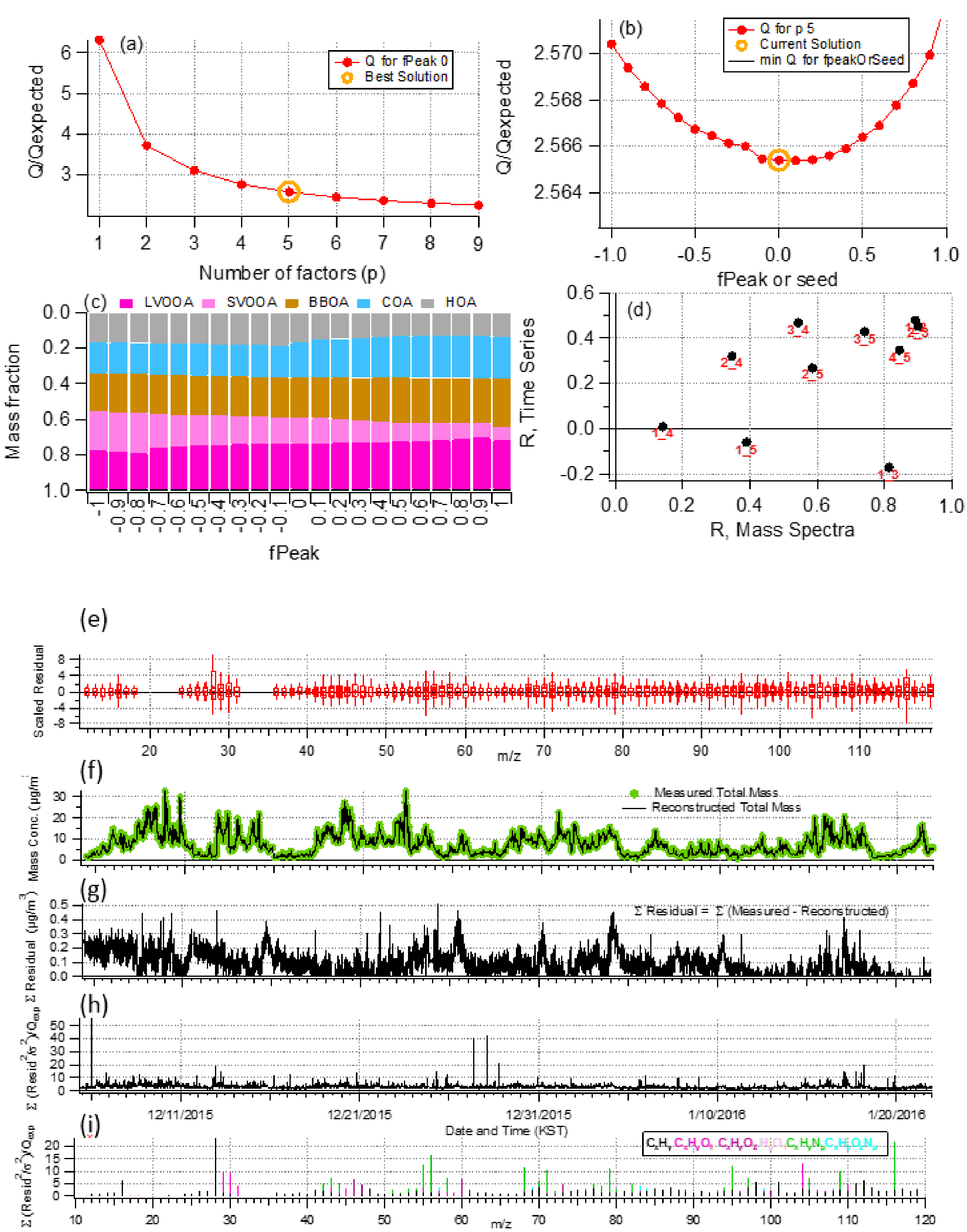

(a)
Q for fPeak 0
Best Solution
Q/Qexpected
Number of factors (p)
(b)
Q for p 5
Current Solution
min Q for fpeakOrSeed
Q/Qexpected
fPeak or seed
(c)
LVOOA
SVOOA
BBOA
COA
HOA
Mass fraction
fPeak
(d)
R, Time Series
R, Mass Spectra
(e)
Scaled Residual
m/z
(f)
Measured Total Mass
Reconstructed Total Mass
Mass Conc. (μg/m³)
(g)
Σ Residual = Σ (Measured - Reconstructed)
Σ Residual (μg/m³)
(h)
Σ (Resid²/σ²)/Q_exp
12/11/2015
12/21/2015
12/31/2015
1/10/2016
1/20/2016
Date and Time (KST)
(i)
Σ (Resid²/σ²)/Q_exp
m/z

Figure S2. Summary of the key diagnostic plots of the chosen 5-factor solution from PMF analysis of the organic aerosol fraction: **(a)** Q/Q_{exp} as a function of the number of factors (*p*) explored in PMF analysis, with the best solution denoted by the open orange circle. Plots **b-i** are for the chosen solution set, containing 5 factors: **(b)** Q/Q_{exp} as a function of fPeak; **(c)** mass fractional contribution to the total OA mass of each of the PMF factors, including the residual (in black), as a function of fPeak; **(d)** Pearson's r correlation coefficient values for correlations among the time series and mass spectra of the PMF factors. Here, 1 = LV-OOA, 2 SV-OOA, 3 = BBOA, 4 = HOA, 5 = COA; **(e)** box and whiskers plot showing the distributions of scaled residuals for each *m/z*; **(f)** time series of the measured organic mass and the reconstructed organic mass from the sum of the five OA factors; **(g)** time series of the variations in the residual (= measured – reconstructed) of the fit; **(h)** the Q/Q_{exp} for each point in time; **(i)** the Q/Q_{exp} values for each fragment ion.

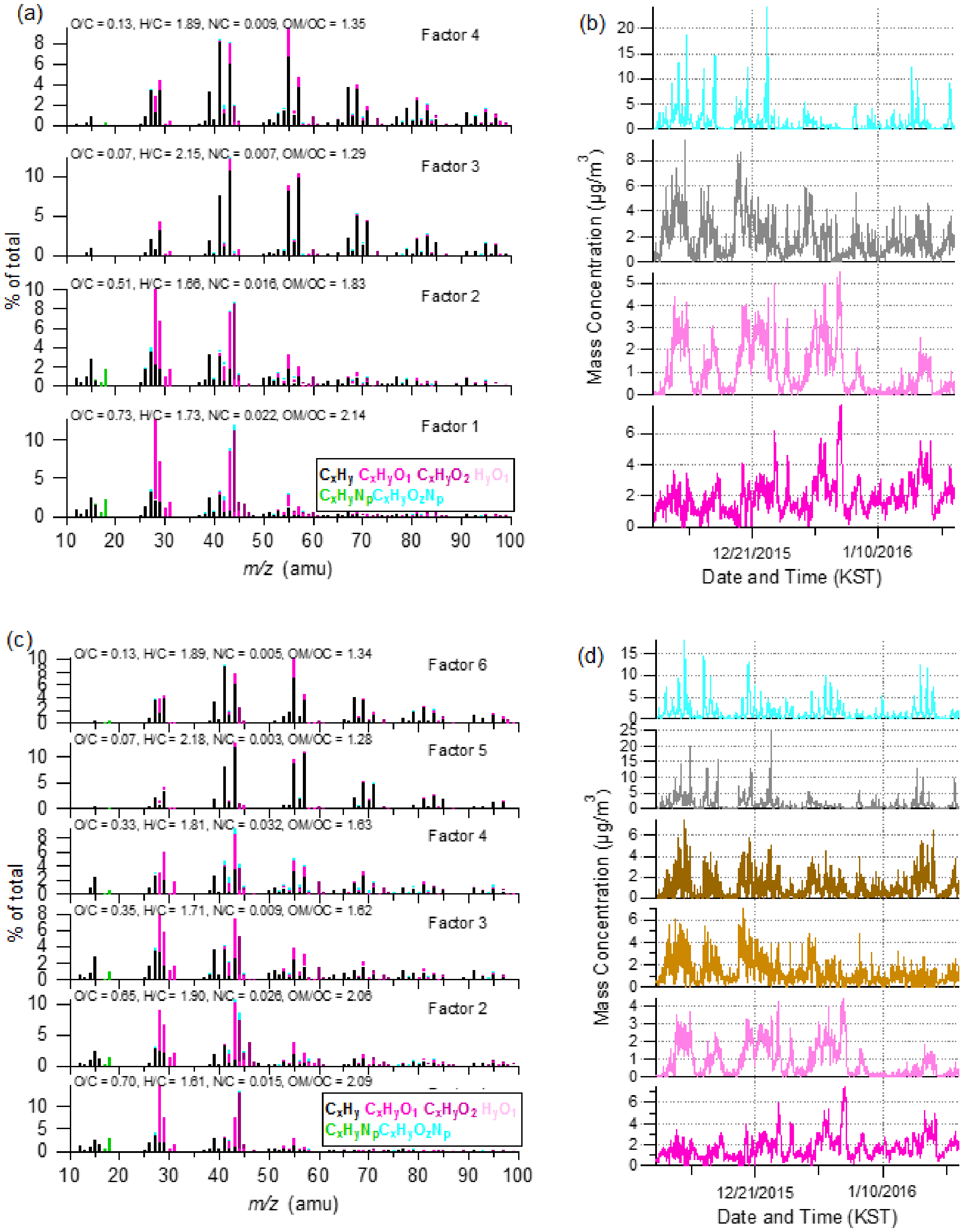

(a)
O/C = 0.13, H/C = 1.89, N/C = 0.009, OM/OC = 1.35
Factor 4
O/C = 0.07, H/C = 2.15, N/C = 0.007, OM/OC = 1.29
Factor 3
O/C = 0.51, H/C = 1.66, N/C = 0.016, OM/OC = 1.83
Factor 2
O/C = 0.73, H/C = 1.73, N/C = 0.022, OM/OC = 2.14
Factor 1
% of total
m/z (amu)
(b)
Mass Concentration (µg/m³)
12/21/2015
1/10/2016
Date and Time (KST)
(c)
O/C = 0.13, H/C = 1.89, N/C = 0.005, OM/OC = 1.34
Factor 6
O/C = 0.07, H/C = 2.18, N/C = 0.003, OM/OC = 1.28
Factor 5
O/C = 0.33, H/C = 1.81, N/C = 0.032, OM/OC = 1.63
Factor 4
O/C = 0.35, H/C = 1.71, N/C = 0.009, OM/OC = 1.62
Factor 3
O/C = 0.65, H/C = 1.90, N/C = 0.026, OM/OC = 2.06
Factor 2
O/C = 0.70, H/C = 1.61, N/C = 0.015, OM/OC = 2.09
% of total
m/z (amu)
(d)
Mass Concentration (µg/m³)
12/21/2015
1/10/2016
Date and Time (KST)

Figure S3. Overview of two other solution sets from PMF analysis: **(a)(b)** High resolution mass spectra and time series of the different OA factors from the 4-factor solution; **(c)(d)** High resolution mass spectra and time series of the different OA factors from the 6-factor solution. The mass spectra are colored by different ion families and the time series are colored by possible factor sources (grey = HOA, blue = COA, brown = BBOA, pink = OOA). See Sect. 2.3.2 in the main manuscript for a discussion on these solution sets.

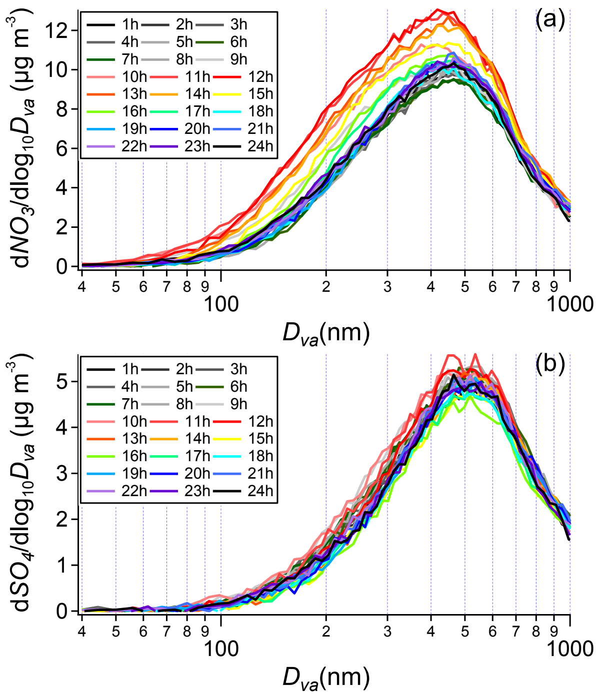

Figure S4. Hourly averaged mass-based size distributions of **(a)** nitrate and **(b)** sulfate during the entire period. Hour shown at legend indicate the diurnal hour of the day.

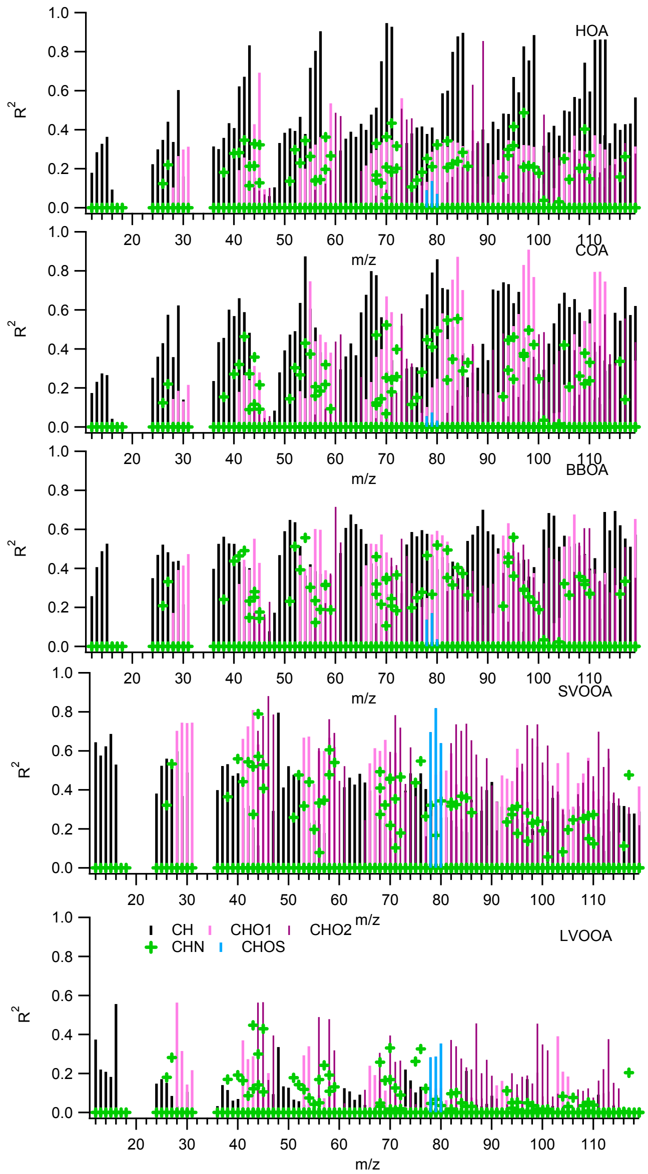

Figure S5. Correlations between five OA factors and HRMS ions that are segregated into five categories ($C_xH_y^+$, $C_xH_yO^+$, $C_xH_yO_2^+$, $C_xH_yN_p^+$ and $C_xH_yO_zS_q^+$).

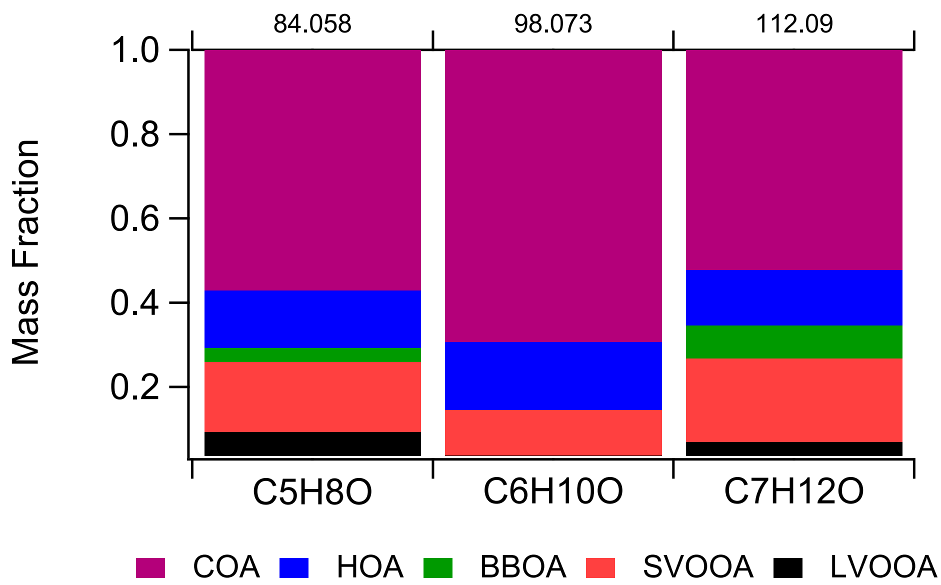

Figure S6. Mass fractional contribution of the five OA factors from PMF analysis to various ions that are relevant to COA tracers.

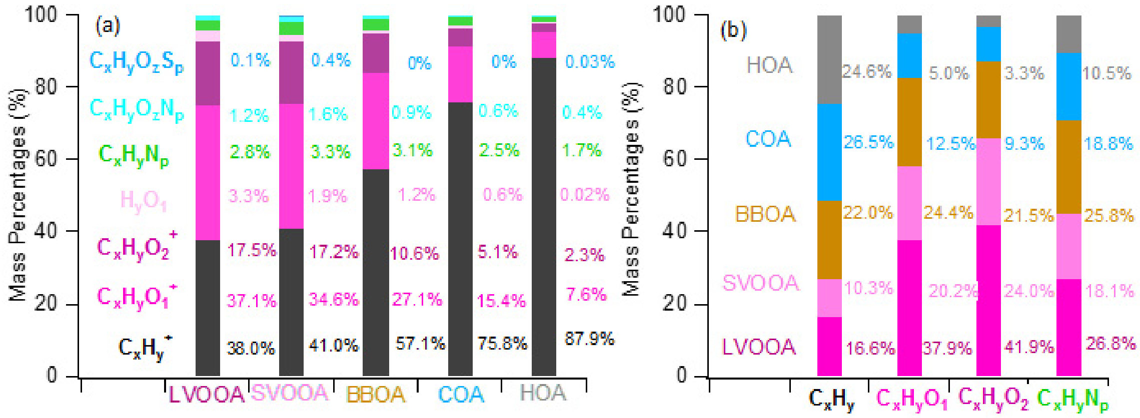

Figure S7. (a) Average mass fractional contributions of seven ion families to each of the OA factors and **(b)** Average mass fractional contributions of five OA factors to 4 each ion families

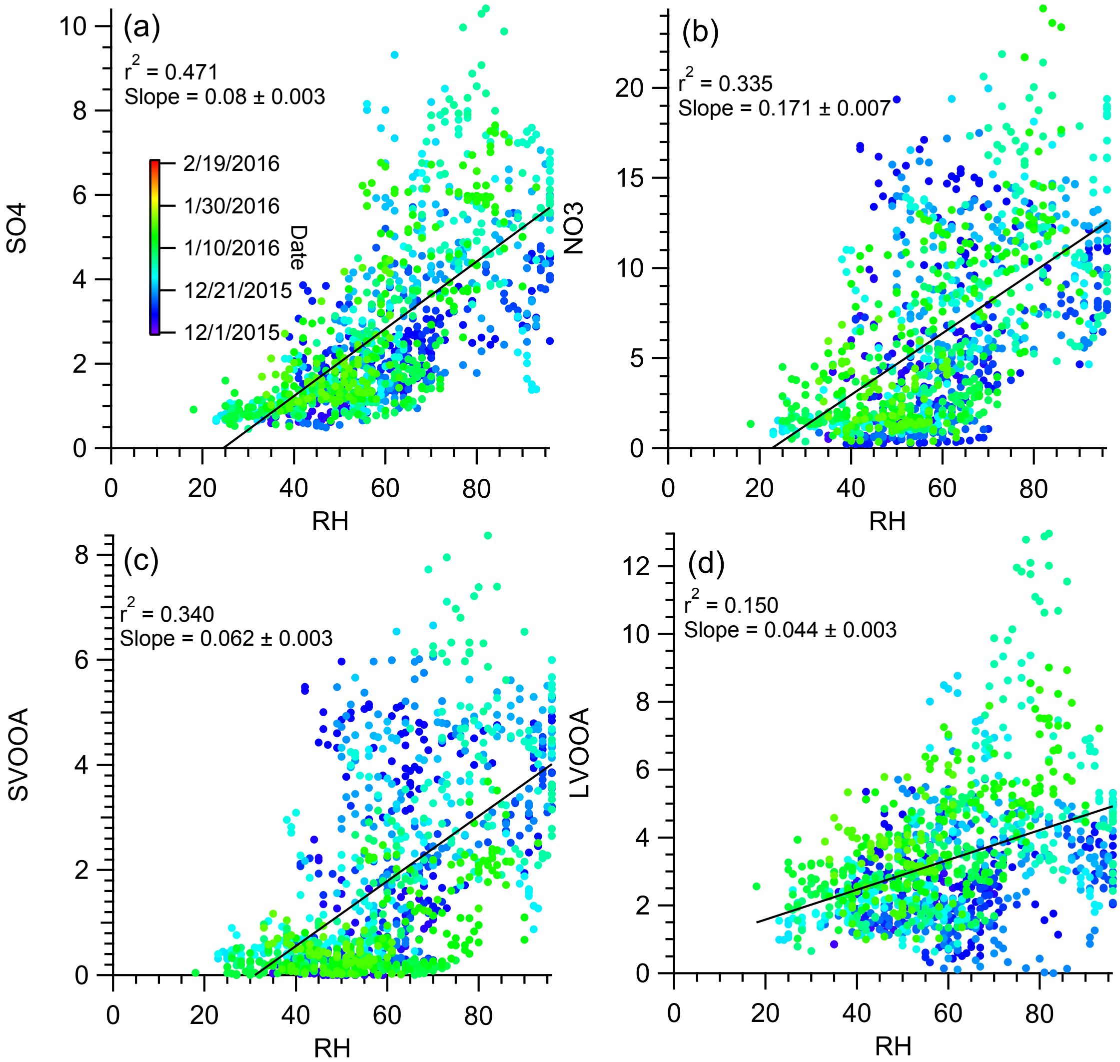

Figure S8. Scatterplot between inorganic compounds: **(a)** sulfate **(b)** nitrate which can be formed by aqueous phase reaction under high RH versus RH; and **(c)** SV-OOA and **(d)** LV-OOA which OA source that can be formed secondarily under high RH.

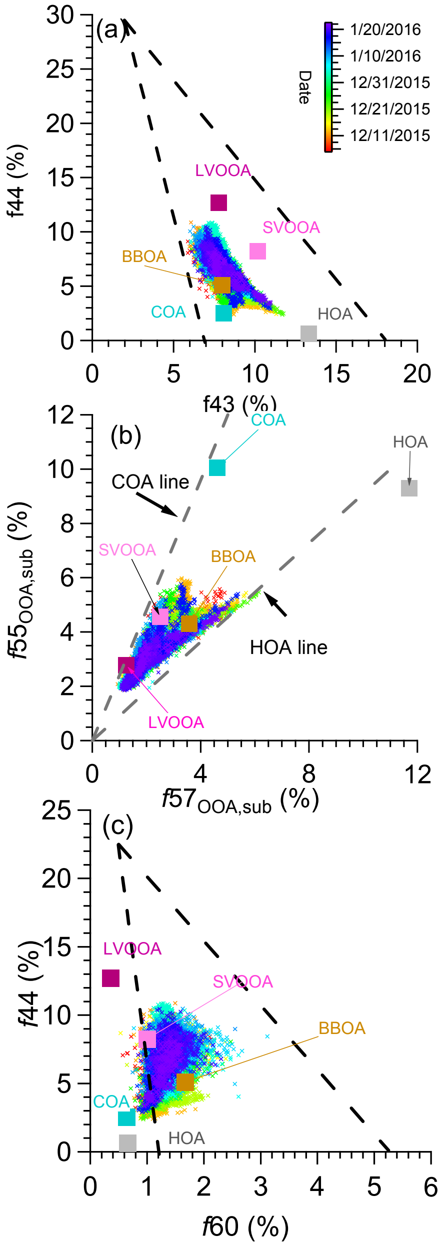

Figure S9. Triangular plots of **(a)** f_{44} versus f_{43} and **(b)** f_{44} versus f_{60} (c) $f_{55,\mathrm{OOA\ sub}}$ versus $f_{57,\ \mathrm{OOA\ sub}}$ for the five OA factors and all of the measured OA data (dots), colored by the time of the day. f_{43}, f_{44}, and f_{60} are the ratios of the organic signal at m/z = 43, 44, and 60 to the total organic signal in the component mass spectrum, respectively. $f_{55,\mathrm{OOA\ sub}}$ and $f_{55,\mathrm{OOA\ sub}}$ are the ratios of the organic signal at m/z 55, 57 after subtracting the contributions from SV-OOA and LV-OOA (e.g., $f_{55,\mathrm{OOA\ sub}} = m/z\ 55 - m/z55_{SV\text{-}OOA} - m/z55_{LV\text{-}OOA}$; $f_{57,\mathrm{OOA\ sub}} = m/z\ 57 - m/z\ 57_{SV\text{-}OOA} - m/z\ 57_{LV\text{-}OOA}$)

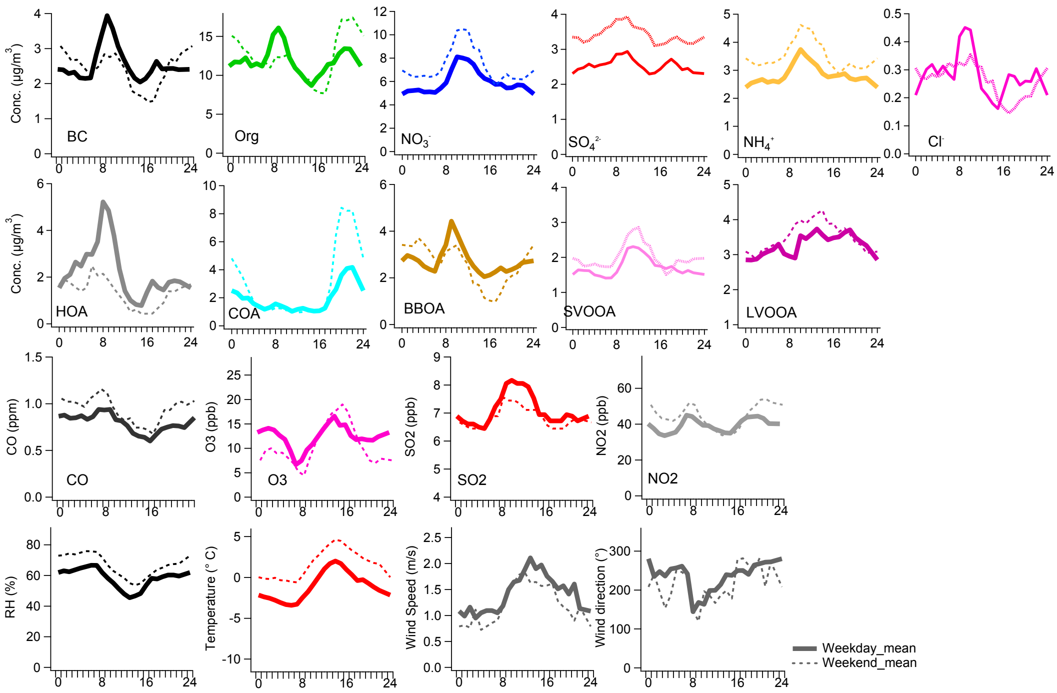

Figure S10. Average diurnal profiles for weekdays (Tuesday to Friday) and weekends (Sunday) for the PM_1 species measured by the aerosol mass spectrometer (AMS) and multi angle absorption photometer (MAAP) (top row), the five OA factors identified from the PMF analysis (second row from the top), various gas phase species (middle row), and various meteorological parameters (bottom row). In this Figure, weekdays were considered to be from Tuesday to Friday, and weekends were only with Sunday. The exclusion of Monday and Saturday was to reduce potential carryover effect as some species, such as nitrate, is possibly influenced by emissions from the previous day (e.g., NO_x). For comparisons, the results from the classification of weekdays as Monday to Friday and weekends as Saturday and Sunday are reported in Fig. S11.

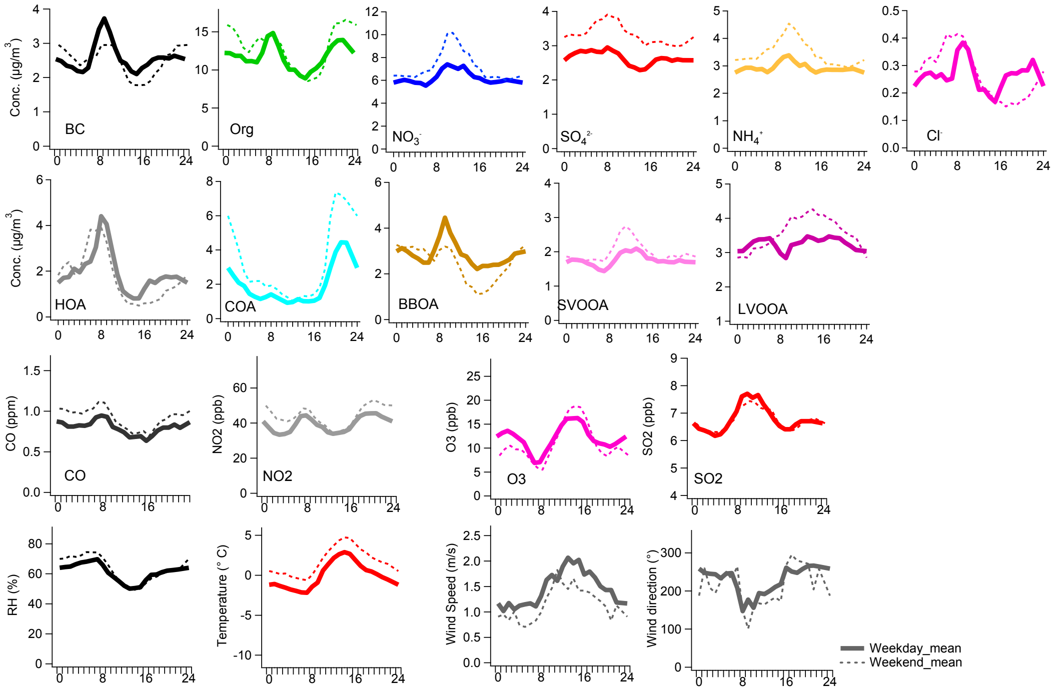

Figure S11. Average diurnal profiles for weekdays (Monday to Friday) and weekends (Saturday, Sunday) for the PM_1 species measured by the aerosol mass spectrometer (AMS) and multi angle absorption photometer (MAAP) (top row), the five OA factors identified from the PMF analysis (second row from the top), various gas phase species (middle row), and various meteorological parameters (bottom row).

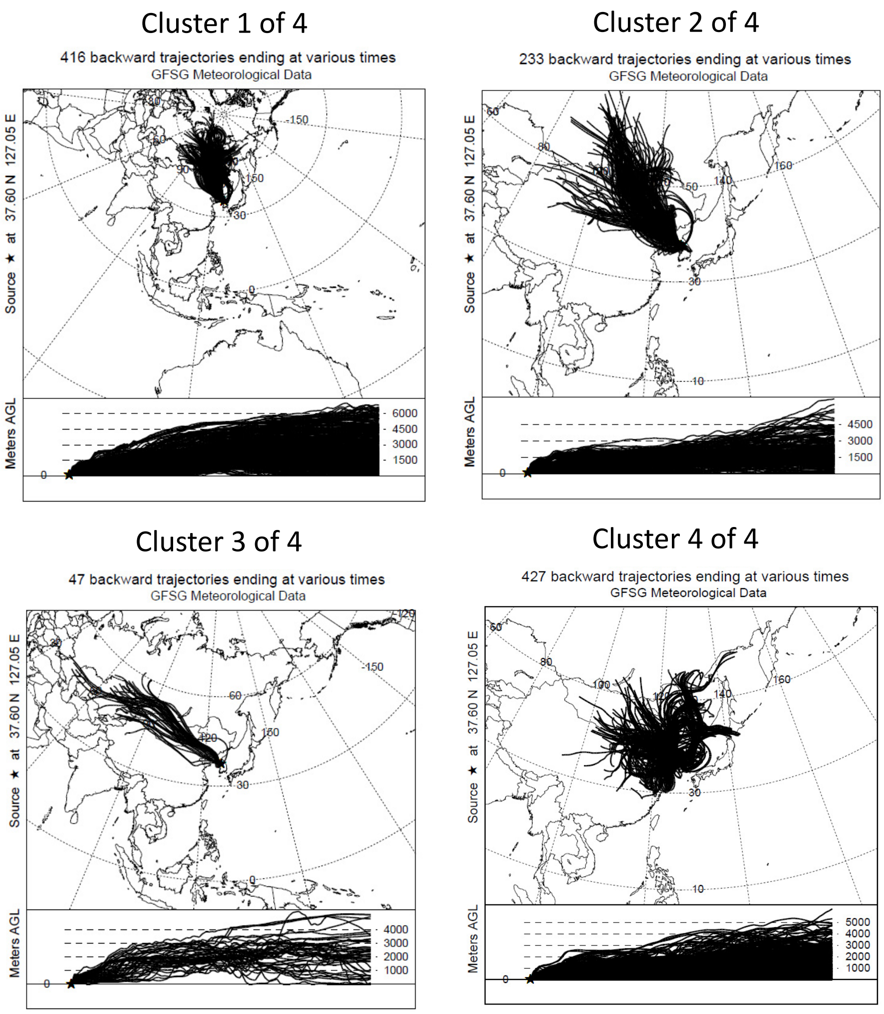

Figure S12. 96 hour back trajectories of air masses arriving at KIST every hour shown on the map for each cluster.

References

Aiken, A. C., Decarlo, P. F., Kroll, J. H., Worsnop, D. R., Huffman, J. A., Docherty, K. S., Ulbrich, I. M., Mohr, C., Kimmel, J. R., Sueper, D., Sun, Y., Zhang, Q., Trimborn, A., Northway, M., Ziemann, P. J., Canagaratna, M. R., Onasch, T. B., Alfarra, M. R., Prevot, A. S. H., Dommen, J., Duplissy, J., Metzger, A., Baltensperger, U., and Jimenez, J. L.: O/C and OM/OC ratios of primary, secondary, and ambient organic aerosols with high-resolution time-of-flight aerosol mass spectrometry, Environmental Science & Technology, 42, 4478-4485, 10.1021/es703009q, 2008.

Canagaratna, M. R., Jimenez, J. L., Kroll, J. H., Chen, Q., Kessler, S. H., Massoli, P., Hildebrandt Ruiz, L., Fortner, E., Williams, L. R., Wilson, K. R., Surratt, J. D., Donahue, N. M., Jayne, J. T., and Worsnop, D. R.: Elemental ratio measurements of organic compounds using aerosol mass spectrometry: characterization, improved calibration, and implications, Atmospheric Chemistry and Physics, 15, 253-272, 10.5194/acp-15-253-2015, 2015.

Kuwata, M., Zorn, S. R., and Martin, S. T.: Using Elemental Ratios to Predict the Density of Organic Material Composed of Carbon, Hydrogen, and Oxygen, Environmental Science & Technology, 46, 787-794, 10.1021/es202525q, 2012.

Middlebrook, A. M., Bahreini, R., Jimenez, J. L., and Canagaratna, M. R.: Evaluation of Composition-Dependent Collection Efficiencies for the Aerodyne Aerosol Mass Spectrometer using Field Data, Aerosol Science and Technology, 46, 258-271, 10.1080/02786826.2011.620041, 2012.

Zhang, Q., Canagaratna, M. R., Jayne, J. T., Worsnop, D. R., and Jimenez, J. L.: Time- and size-resolved chemical composition of submicron particles in Pittsburgh: Implications for aerosol sources and processes, Journal of Geophysical Research-Atmospheres, 110, 10.1029/2004jd004649, 2005.